Estimation of rock Fe content based on hyperspectral indices (Postprint)

Authors: Jinlin Wang, WANG Wei, CHENG Yinyi, ZHANG Zhixin, WANG Shanshan, ZHOU Kefa, LI Pingheng, WANG Wei

Date: 2021-12-30T18:54:44+00:00

Abstract

Information on the Fe content of bare rocks is needed for implementing geochemical processes and identifying mines. However, the influence of Fe content on the spectra of bare rocks has not been thoroughly analyzed in previous studies. The Saur Mountain region within the Hoboksar of the Russell Hill depression was selected as the study area. Specifically, we analyzed six hyperspectral indices related to rock Fe content based on laboratory measurements (Dataset I) and field measurements (Dataset II). In situ field measurements were acquired to verify the laboratory measurements. Fe content of the rock samples collected from different fresh and weathered rock surfaces were divided into six levels to reveal the spatial distributions of Fe content of these samples. In addition, we clearly displayed wavelengths with obvious characteristics by analyzing the spectra of these samples. The results of this work indicated that Fe content estimation models based on the fresh rock surface measurements in the laboratory can be applied to in situ field or satellite-based measurements of Fe content of the weathered rock surfaces. It is not the best way to use only the single wavelengths reflectance at all absorption wavelengths or the depth of these absorption features to estimate Fe content. Based on sample data analysis, the comparison with other indices revealed that the performance of the modified normalized difference index is the best indicator for estimating rock Fe content, with R2 values of 0.45 and 0.40 corresponding to datasets I and II, respectively. Hence, the modified normalized difference index (the wavelengths of 2220, 2290, and 2370 nm) identified in this study could contribute considerably to improve the identification accuracy of rock Fe content in the bare rock areas. The method proposed in this study can obviously provide an efficient solution for large-scale rock Fe content measurements in the field.

Full Text

Preamble

Estimation of rock Fe content based on hyperspectral indices

WANG Jinlin[1,2,3,4], WANG Wei[1,2,3,4*], CHENG Yinyi[1,2,3,4], ZHANG Zhixin[1,2,3,4], WANG Shanshan[1,2,3,4], ZHOU Kefa[1,2,3,4], LI Pingheng[5]

[1]State Key Laboratory of Desert and Oasis Ecology, Xinjiang Institute of Ecology and Geography, Chinese Academy of Sciences, Urumqi 830011, China

[5]Zhejiang A & F University, Hangzhou 311300, China

Abstract: Information on the Fe content of bare rocks is needed for implementing geochemical processes and identifying mines. The Saur Mountain region within the Hoboksar of the Russell Hill depression was selected as the study area. We analyzed six hyperspectral indices related to rock Fe content based on laboratory measurements (Dataset I) and field measurements (Dataset II). In situ field measurements were acquired to verify the laboratory measurements. Fe content of the rock samples collected from different fresh and weathered rock surfaces were divided into six levels to reveal the spatial distributions of Fe content of these samples. In addition, we clearly displayed wavelengths with obvious characteristics by analyzing the spectra of these samples. The results of this work indicated that Fe content estimation models based on fresh rock surface measurements in the laboratory can be applied to in situ field or satellite-based measurements of Fe content of weathered rock surfaces. It is not the best way to use only the single-wavelength reflectance at all absorption wavelengths or the depth of these absorption features to estimate Fe content. Based on sample data analysis, the comparison with other indices revealed that the performance of the modified normalized difference index is the best indicator for estimating rock Fe content, with R^2 values of 0.45 and 0.40 corresponding to datasets I and II, respectively. Hence, the modified normalized difference index (the wavelengths of 2220, 2290, and 2370 nm) identified in this study could contribute considerably to improving the identification accuracy of rock Fe content in bare rock areas. The method proposed in this study can obviously provide an efficient solution for large-scale rock Fe content measurements in the field.

Keywords: bare rocks; Fe content; reflectance; spectral indices; modified normalized difference index; Saur Mountain

1 Introduction

Iron (Fe) minerals in rocks play a pivotal role in geochemical investigations; for this reason, it is necessary to monitor Fe content of rocks in extensive areas (Baugh et al., 1998; Velasco et al., 2005; Li et al., 2009; Liu et al., 2010; Simandl and Paradis, 2018). Conventionally, local measurements are an important means for determining Fe content of rocks, and extrapolating the measured value from each sampling point is helpful for deriving maps of rock Fe content

(Liu et al., 2016). Application of remote sensing technology to obtain the feature information of rocks has the advantages of wide coverage and fast speed (Hao et al., 2019; Zeraatpisheh et al., 2019). Furthermore, some scholars have emphasized that the optical domain can be used for such researches (Galvao et al., 2008; Middleton et al., 2011; Nair and Mathew, 2012; Metelka et al., 2015; Qian et al., 2019). Accordingly, the retrieval of hyperspectral images provides a new approach for extracting surface information (Clark and Roush, 1984; van der Meer, 2018).

However, classic remote sensing instruments (such as the ASTER and Landsat platforms) cannot effectively retrieve surface characteristics of rocks because it is difficult to analyze their diagnostic spectral characteristics within the wavelengths of 100–200 nm bands (Clark and Roush, 1984; Wu et al., 1997; Liu and Vekerdy, 2003). In contrast, hyperspectral indices, e.g., leaf area index (LAI), chlorophyll concentration, and other plant pigments (Rathod et al., 2016), plant water content (Pour et al., 2019), soil moisture (Sarathjith et al., 2016), and soil salinity (Jia et al., 2021), exhibit very good performance at acquiring information on vegetation and soil characteristics. Nevertheless, although some scholars have employed hyperspectral technology to quantitatively determine the contents of rock elements, few have leveraged this potential well (Sracek et al., 2004; Gasmi et al., 2018).

Rock reflectance has been shown to be affected by Fe content in the wavelengths of 2000–2500 nm. Although some studies have indicated that the general trend of rock spectral reflectance changes with variation in rock Fe content, some other results suggested that rock Fe content can be precisely estimated by hyperspectral data (Clénet et al., 2011). However, this theory is not yet fully understood with regard to the estimation of bare rock element contents, and this method has a strong innovation in remote sensing application. Due to the differences of Fe content in different rock types, spectral absorption should be fully considered in the estimation of rock Fe content (Clark et al., 2003; Wang et al., 2019). Rocks are composed of many different materials containing various kinds of minerals. Hence, the reflectivity of rocks depends on the inherent scattering and absorption characteristics of the components and arrangement of rocks; consequently, the influence of rock Fe content on the reflectance spectrum cannot be accurately described (Chabrillat et al., 2002). This study is one of the first to evaluate Fe content of rocks using hyperspectral data.

The main purposes of this study were: (1) to explore both the variations in rock Fe content in the field and the changes in the spectral reflectance at six wavelength levels; (2) to identify hyperspectral indices of rock Fe content that are insensitive to other rock components; and (3) to develop a method for estimating Fe content in the field using an optimized Fe content hyperspectral index. To achieve these goals, we conducted field surveys as experiments, obtained spectral data by collecting bare rock samples and analyzing Fe content in the laboratory, and measured and analyzed the spectra characteristics of the samples. The results are of great practical significance for the determination of

rock Fe content.

2.1 Study area

The study area is located in the Saur Mountain region within the Hoboksar of the Russell Hill depression (46°25 −46°52 N, 85°00 −86°15 E). This area has a continental climate, with wide temperature range and sparse vegetation coverage. There are a large number of exposed rocks at the selected sampling points. The study area contains evidence of coal, copper, siderite, magnetite, limonite, titanium magnetite, chromite, pyrite, fluorite, clays, and other minerals in a total of 40 useful deposits, and five diffusion halos are discovered comprising numerous beneficial minerals (elements), including zircon, hafnium zircon, chromium, nickel, and cobalt.

2.2 Reflectance measurements

Both weathered surfaces and fresh surfaces were used for reflectance measurements. Reflectance spectra were measured in situ for each sample using an Analytical Spectral Device (ASD) FieldSpec FR spectrometer (American Analytical Spectral Instruments Company, Tucson, USA), covering wavelengths from 350 to 2500 nm at an interval of 1 nm. The key sampling area was determined in combination with remote sensing images and geological data. A total of 313 rock (81 samples) and mineral (232 samples) samples were collected. The rock reflectance spectra were measured in situ within the period from 10:00 to 14:00 (LST) during 3 August–21 September in 2019 under cloud-free conditions with a 25° fiber optic. In each measurement, the radiance and reflectance were converted using the "reflectance spectrum" function on the panel. These in situ field reflectance data were denoted as Dataset II.

All spectral measurements were conducted in a completely dark room to avoid contamination by other light sources. This laboratory reflectance data were denoted as Dataset I. We further divided the laboratory and field sample data according to the degree of weathering. Specifically, Reflectance-Laboratory-Old refers to the weathered surface in the laboratory, Reflectance-Laboratory-New refers to the fresh surface in the laboratory, Reflectance-Field-Old refers to the weathered surface in the field, and Reflectance-Field-New refers to the field fresh surface.

After acquiring the field spectral measurements, the rock samples were transported to the laboratory; then, the surface reflectance of each rock sample was again measured using the ASD FieldSpec FR spectrometer. A tungsten quartz halogen filament lamp was used to illuminate the rock samples from 50 cm away, and the beam was oriented 30° from the vertical. The reflected light was collected perpendicular to the sample with a 5° field of view at a distance of 10 cm. We carried out measurement experiments in a completely dark laboratory to avoid the effects of other light sources. Based on the results of 81 rock samples, we classified Fe content into six levels: 0.00%–1.00% (Level 1), 1.00%–2.00%

(Level 2), 2.00%-3.00% (Level 3), 3.00%-4.00% (Level 4), 4.00%-5.00% (Level 5), and >5.00% (Level 6).

2.3 Continuum removal analysis

To analyze the effects of Fe content on rock reflectance, we clearly displayed the absorption characteristics in the rock reflection spectrum by optimizing the continuous measurement spectrum (Clark and Roush, 1984). This method was the first to recommend employing a continuum removal analysis to distinguish individual absorption features of interest. The continuum is a convex "hull" fitted to the straight-line segments at the top of the spectrum. These spectral segments are connected to the local spectral maximum and represent the "background" absorption. The other absorption features are then superimposed on the background. The continuum can be removed by dividing the reflectance value of each point in the absorption feature using the reflectance level along the convex hull at the corresponding wavelength.

2.4 Calculation and determination of the best spectral index

This research employed six spectral indices to quantify Fe content, as described in Table 1 . First, according to datasets from the field experiment, we performed correlation analysis to screen the combined wavelengths to determine the best wavelength for each index, and then applied Dataset II to verify the results of the previous step to determine the optimal index category and the most suitable wavelength. The screening step was 5 nm, and the indices were calculated for each combination.

Correspondingly, linear and multiple regression analysis methods can be used to determine the relationship between rock Fe content and reflectivity, and thus predict rock Fe content. In this study, the model used to estimate Fe content was verified from the aspects of stability and prediction capacity. Stability was tested with the adjusted coefficient of determination (R^2) while prediction capacity was judged with the root-mean-square error (RMSE). R^2 and RMSE indicate the effect of the model. The higher the R^2 value is, the higher the stability of the model; the smaller the RMSE value is, the higher the accuracy of the model. In addition, the relative RMSE (average of the RMSE of Fe content; %) was used to evaluate the accuracy of the regression model.

Table 1 Descriptions of the generic types of indices

Index	Formula	Reference
Reflectance difference index	$ 1–ρ 2|*LeMaireetal.*(2004)||*SimpleRatio*ρ 2/ρ 1|*LeMaireetal.*(2008)||*Normalizeddif*ρ 2)|*Wangetal.*(2011)||*Modifiedsimpleratio*|(ρ 1–ρ 2)/(ρ 1+ ρ 2–2ρ 3)|*SimsandGamon*(2002)||*Modifiednormalizeddifferenceindex*|(ρ 1–ρ 3)/(ρ 2	

Note: refers to the reflectance value in the experiment; $ $1, $ $2, and $ $3 represent wavelengths.

Relative RMSE (%) = RMSE / $\bar{y}$, where $\bar{y}$ is the mean value; yj is the independent reference measurement; and n is the number of samples.

3.1 Variation in Fe content of rock samples

Fe content of 81 rock samples varied greatly, ranging from 0.24% to 8.37%, with an average of 2.26% and a standard deviation of 1.62%. As mentioned earlier, we divided Fe content into six levels: 0.00%-1.00% (Level 1), 1.00%-2.00% (Level 2), 2.00%-3.00% (Level 3), 3.00%-4.00% (Level 4), 4.00%-5.00% (Level 5), and >5.00% (Level 6). As can be seen from Figure 1a

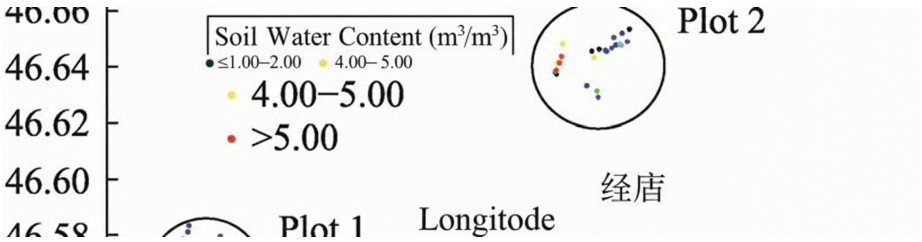

Figure 1: Figure 1

, Fe content of 81 rock samples can be categorized into three plots. Rock Fe content exhibited broad spatial variability, especially in Plot 1. As shown in Figure 1a, the samples in Plot 1 were concentrated, but Fe content of these samples varied from Level 1 to Level 6. In addition, for Plot 2 and Plot 3, Fe content of the samples was also relatively concentrated.

Level 2 had the largest number of samples, followed by levels 1 and 3, while levels 4-6 contained the fewest samples (Fig. 1b). As shown in Figure 1b, all of the rock samples in Plot 3 belonged to levels 1-3, except for one sample belonging to Level 5, while a total of 15 samples in Plot 1 and Plot 2 belonged to levels 4-6.

3.2 Spectral properties of rock samples

For all four reflectance groups (the reflectance of fresh and weathered rock surfaces was measured in the laboratory and in the field), the measured average spectra of all 81 rock samples displayed similar characteristics, with obvious shoulder peaks at 800 nm wavelength and obvious absorption characteristics at wavelengths of 1400, 1900, 2250, and 2350 nm (Fig. 2

). The depth and width characteristics of the absorption wavelengths at 1900 and 2350 nm were more obvious than those of the other two wavelengths (1400 and 2250 nm). The absorption characteristics at wavelengths of 2000 and 2050

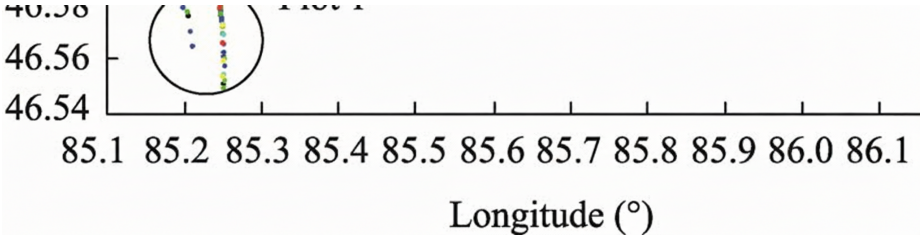

Figure 2: Figure 2

nm measured in the field were clearly weaker than those measured in the laboratory. Moreover, the reflectance values measured in the field were larger than those obtained in the laboratory for both fresh and weathered rock surfaces. By comparing the spectra between the fresh and weathered rock surfaces, it was found that they exhibited almost identical reflectance data at wavelengths of 350–1000 nm, and the fresh rock surfaces had larger reflectance values than the weathered rock surfaces at wavelengths of 1000–2500 nm.

When the rock Fe content was divided into six levels, the spectra also varied among these levels, especially the absorption features at wavelengths of approximately 2250 and 2350 nm (Fig. 1). The depths of the absorption features at these two wavelengths increased when Fe content increased, especially in Level 6. After utilizing the continuum removal method, the characteristics became more obvious. The amplitude of the absorption feature at the wavelength of approximately 2250 nm was small, while that of the absorption feature at the wavelength of approximately 2350 nm was much larger. The relative depth difference of the absorption characteristics between Level 1 and Level 2 was small near 2350 nm, while the depths of the absorption characteristics in levels 3–5 were more obvious. Further, Level 6 had the greatest depth of the absorption characteristics (approximately twice as deep as the other depths) at this absorption wavelength.

3.3 Results of spectral indices

Table 2 shows the validation of Dataset II based on Dataset I through the reflection wavelength with the highest R^2 and the lowest RMSE. Values of R^2 and RMSE for the two datasets were verified, and the model for predicting Fe content was calibrated using Dataset I.

Table 2 Results of the general types of indices calibrated with Dataset I and validated with Dataset II for the estimation of rock Fe content

Index	Wavelength (nm)	Fe = e^(a+b×index)	Dataset I	Dataset II
			R^2	RMSE

Index	Wavelength (nm)	Fe = e^(a+b×index)	Dataset I	Dataset II
Fresh surface				
mND	2220, 2290, 2370		0.45	1.24
Weathered surface				
mND	2220, 2290, 2370		0.40	1.26

Note: "* ", significance level at $P<0.05$; Dataset I, laboratory measurements; Dataset II, in situ field measurements; R^2, coefficient of determination; RMSE, root-mean-squared error; Relative RMSE, relative root mean-squared error; mND, modified normalized difference index.

For the fresh rock surfaces, the reflectance index at 2210 nm exhibited the lowest R^2 (0.05) and the highest RMSE (1.64) based on both datasets by comparing the six indices. For Dataset I, the performance of the reflectance difference index was moderate (the best wavelengths of 2220–2240 nm, R^2=0.29, and RMSE=1.47), but for Dataset II, its performance was slightly lower (R^2=0.25 and RMSE=1.55). Through experimental calculations and analysis, the performance of the best normalized difference index at 2250 and 2350 nm was relatively excellent (R^2=0.41 and R^2=0.38 for datasets I and II, respectively). The performance of the best simple ratio index was similar to that of the best normalized difference index, with the same wavelengths and only slightly lower accuracy (R^2=0.40 and R^2=0.37 for datasets I and II, respectively).

The modified normalized difference index (the wavelengths of 2220, 2290, and 2370 nm) performed best among the six indices, with R^2 values of 0.45 and 0.39 and RMSE values of 1.24 and 1.34 for datasets I and II, respectively. The best modified simple ratio index yielded a similar result to the best modified normalized difference index, with three wavelengths at 2210, 2250, and 2360 nm, although the accuracy was slightly lower (R^2=0.42 and RMSE=1.26 for Dataset I and R^2=0.38 and RMSE=1.37 for Dataset II).

Measurements of the weathered rock surfaces were consistent with those of the fresh rock surfaces for all six indices. The best indicator for the weathered rock surfaces was the modified normalized difference index, with R^2 value of 0.40 and RMSE value of 1.26 for Dataset I; however, for Dataset II, its performance was slightly reduced, with R^2 value of 0.38 and RMSE value of 1.37. This index had the same wavelengths for the weathered rock surfaces as that for the fresh rock surface measurements, and the accuracy was similar, albeit just slightly lower than the wavelengths of the fresh rock surface counterpart. However, it is worth noting that the regression coefficient was unstable and its range varied between the fresh and weathered rock surfaces.

In the experiment of estimating rock Fe content, the determined index was used in the exponential regression equation. We used the estimated Fe content and the measured data to construct the scatter plots, as shown in Figure 3

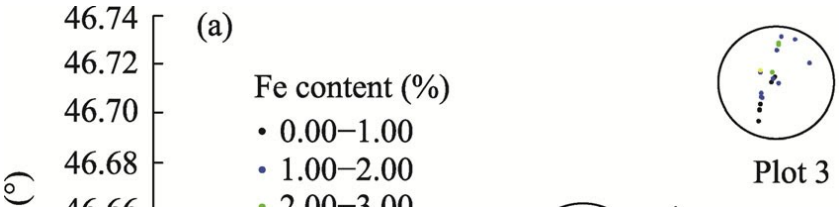

Figure 3: Figure 3

. It can be seen that most of the data points were distributed along the 1:1 line, which suggested that this index had good performance for both field and laboratory measurements.

4.1 Spectral properties of rock samples

Although there are many high-quality optical remote sensing instruments in orbit, few scientific investigations were conducted using different wavebands (including visible light, far-near infrared, and/or hyperspectral instruments) to accurately estimate the mineral (element) contents in rocks, including Fe content. This is because electromagnetic waves cannot completely penetrate clouds and vegetation canopy and are further affected by atmospheric factors. The factors influencing the measurements of rock reflectivity include not only Fe content but also contents of other elements in rocks, the physical structure of rocks, and the observation conditions and methods. Due to these reasons, the observations of Fe content in mixed rock samples are biased. In this research, the conditions of the natural arid environment of western China, including the measurable bare rocks, sparse vegetation, and relatively cloudless skies, are all conducive to calculating Fe content of rocks in the study area.

The results of rock measurements by previous researchers in different environments have shown that Fe ions have major absorption features at wavelengths of 2260 and 2350 nm (van der Meer et al., 2014). It has also been found that the depth of these absorption features increases with increasing rock Fe content (van der Meer et al., 2014), which is consistent with the results reported in this study. Specifically, as shown in Figure 2, when Fe content level increased, the depth of the absorption features at wavelengths of 2260 and 2350 nm increased monotonically. However, when using only the single-band reflectance at these absorption wavelengths or the depth of these absorption features to estimate Fe content, the result was not ideal. This may be because the effect of Fe content on rock reflectance is weak, nonlinear, and complicated. Furthermore, this effect is influenced by interference due to other elements, such as magnesium (Rowan et al., 2004). Therefore, rock Fe content must be identified from hyperspectral

indices that are insensitive to other factors.

4.2 Hyperspectral indices to estimate rock Fe content

Due to differences in applications, some multispectral indices are designed to be insensitive to changes in some spectra. For example, the reflectance difference index is not sensitive to the cumulative change in reflectance, while the simple ratio and normalized difference index are not sensitive to the proportional effect. Additionally, the modified simple ratio and modified normalized difference index are insensitive to both additive and proportional effects (Le Maire et al., 2008). Referring to Dataset I, the result indicates that the performance of the modified normalized difference index and modified simple ratio is better than that of the simple ratio, normalized difference, and reflectance difference index, and the index efficiency considering both the additive effect and the proportional effect will be better than the index efficiency considering only one effect. The same is true for Dataset II. The results obviously demonstrate that more complex indices, such as the modified simple ratio and modified normalized difference index, are better than the other simple indices, which may be because the indices using three wavelengths contain more information and thus are more sensitive to other rock properties than those using two wavelengths. Therefore, these higher-complexity indices are more appropriate for devising more efficient indices.

Hyperspectral indices are widely used in retrieving vegetation and soil properties (Zeng et al., 2021). However, few studies have used this approach to estimate the bare rock Fe content. This study aims to develop an optimal hyperspectral index for estimating rock Fe content that is feasible for both laboratory and in situ field measurements. The best indicator that was identified in this research work is the modified normalized difference index, which demonstrates the best performance with both laboratory-based and field-based measurements. Furthermore, as shown in Table 2 and Figure 3, the modified normalized difference index (2220, 2290, and 2370 nm) performed consistently among the different datasets and rock surfaces (fresh and weathered rock surfaces), although there was a small decrease in R^2 for Dataset II from the weathered rock surfaces.

4.3 Reflectance of weathered and fresh rock surfaces measured in laboratory and field

A large calibration dataset is very important to obtain general indices. Because of cost constraints, a restricted research area can have a substantial impact on the experimental design and field measurements; as a result, it is impossible to provide a more accurate comprehensive field dataset, and only the index method suitable for the current research area can be used. By contrast, fitting experimental datasets to actual field-measured spectra can provide an alternative solution to find a suitable index. However, to use laboratory datasets instead of field measurements, the laboratory-measured rock reflectance spectra must

completely match the field-measured spectra.

Under general conditions, based on the measured spectra, the matching results between the laboratory and field spectra are not very satisfactory. The experimental results of this research prove the feasibility of the proposed method, which accurately describes the correlation of the rock reflectance spectra measured in the laboratory and in the field. Consequently, some characteristic wavelengths can be identified with the proposed method (for example, the 2000–2100 nm wavelengths), and the field-measured reflectance is always larger than the laboratory-measured reflectance at all optical wavelengths. Therefore, all regression models based on the laboratory datasets may need to be recalibrated before being applied in the field. Thus, extending actual spectral data obtained in the field by using spectral data from the laboratory is an excellent solution. However, due to the shortcomings of this approach, it is difficult to find suitable accurate indicators, so the comprehensive utilization of laboratory and field data can verify and calibrate the final results.

In recent years, the methods employed to accurately and quantitatively determine rock Fe content are unable to combine laboratory measurements with in situ field measurements (Moumane et al., 2021). In this research, two datasets comprising laboratory measurements and field measurements were comprehensively utilized, and the correlations between bare rock Fe content and spectral indices were accurately and extensively described and tested.

Many laboratory measurements use the fresh rock surfaces of rock samples, but in situ field measurements and satellite-borne sensors have access only to the weathered rock surfaces when obtaining reflectance information. In this study, we measured the reflectance of experimental samples from both weathered and fresh rock surfaces to detect the difference between the two types of surfaces. The results indicate that the patterns of the reflectance curves of the two types of surfaces were almost the same not only for the laboratory datasets but also for the field datasets; the only difference was that the reflectance of the weathered rock surfaces was slightly higher than that of the fresh rock surfaces. The best Fe content estimation indices for these two surfaces were also the same (Table 2), and the accuracy was just slightly lower for the weathered rock surfaces than for the fresh rock surfaces (the best R^2 values of 0.45 and 0.40 for the fresh and weathered rock surfaces, respectively). This small error is to be expected and acceptable, as the weathered rock surfaces always have adventitious materials, which will affect the estimation accuracy of Fe content. The outcomes of this work indicate that Fe content estimation models based on the fresh rock surface measurements in the laboratory can be applied to the field or satellite measurements of the weathered rock surfaces.

5 Conclusions

This study assessed the use of hyperspectral indices for estimating bare rock Fe content. The longwave-infrared domain (1100–2526 nm) is suitable for predict-

ing rock Fe content, especially at two or more characteristic wavelengths, which is somewhat obvious. The best indicator for estimating rock Fe content in the field is the modified normalized difference index (2220, 2290, and 2370 nm), a commonly used spectral parameter that can accurately and quickly measure Fe content in bare rocks. The method proposed in this study can obviously provide an efficient solution for large-scale rock Fe content measurements in the field. In order to improve the accuracy of measuring rock Fe content, it is necessary to accurately describe the correlation between Fe content and reflectivity in rocks and to ascertain how different characteristics of rocks and elemental contents in rocks affect their Fe content.

Acknowledgements: This study was funded by the Xinjiang Science and Technology Major Project (2021A03001-3), the National Key R&D Program of China (2018YFC0604001-3), the B&R Team of Chinese Academy of Sciences (2017-XBZG-BR-002), and the National Natural Science Foundation of China (U1803117, U1803241).

References

Baugh W M, Kruse F A, Atkinson Jr W W. 1998. Quantitative geochemical mapping of ammonium minerals in the southern Cedar Mountains, Nevada, using the Airborne Visible/Infrared Imaging Spectrometer (AVIRIS). Remote Sensing of Environment, 65(3): 292–308.

Chabrillat S, Goetz A F H, Krosley L, et al. 2002. Use of hyperspectral images in the identification and mapping of expansive clay soils and the role of spatial resolution. Remote Sensing of Environment, 82(2–3): 431–445.

Clark R N, Roush T L. 1984. Reflectance spectroscopy: Quantitative analysis techniques for remote sensing applications. Journal of Geophysical Research, 89(B7): 6329–6340.

Clark R N, Gregg A, Swayze K, et al. 2003. Imaging spectroscopy: Earth and planetary remote sensing with the USGS Tetracorder and expert systems. Journal of Geophysical Resources, 108(E12): 5131–5144.

Clénet H, Pinet P, Daydou Y, et al. 2011. A new systematic approach using the Modified Gaussian Model: Insight for the characterization of chemical composition of olivines, pyroxenes and olivine-pyroxene mixtures. Icarus, 213(1): 404–422.

Galvao L S, Formaggio A R, Couto E G, et al. 2008. Relationships between the mineralogical and chemical composition of tropical soils and topography from hyperspectral remote sensing data. ISPRS Journal of Photogrammetry and Remote Sensing, 63(2): 259–271.

Gasmi A, Gomez C, Lagacherie P, et al. 2018. Surface soil clay content mapping at large scales using multispectral (VNIR–SWIR) ASTER data. International Journal of Remote Sensing, 40(4): 1506–1533.

Hao L, Zhang Z, Yang X. 2019. Mine tailing extraction indexes and model using remote-sensing images in southeast Hubei Province. Environmental Earth Sciences, 78: 493, doi: 10.1007/s12665-019-8439-1.

Jia X Y, O' Connor D, Shi Z, et al. 2021. VIRS based detection in combination with machine learning for mapping soil pollution. Environmental Pollution, 268: 115845, doi: 10.1016/j.envpol.2020.115845.

Le Maire G, Francois C, Dufrene E. 2004. Towards universal broad leaf chlorophyll indices using PROSPECT simulated database and hyperspectral reflectance measurements. Remote Sensing of Environment, 89(1): 1–28.

Le Maire G, François C, Soudani K, et al. 2008. Calibration and validation of hyperspectral indices for the estimation of broadleaved forest leaf chlorophyll content, leaf mass per area, leaf area index and leaf canopy biomass. Remote Sensing of Environment, 112(10): 3846–3864.

Li H, Lin Q Z, Liu Q J, et al. 2009. Feasibility research on estimating geochemistry element abnormity based on reflectance spectrum of gold deposit in Hatu-Baogutu. Remote Sensing Applications, 8: 43–49.

Liu B, Jin H, Sun Z, et al. 2016. Geochemical weathering of aeolian sand and its palaeoclimatic implications in the Mu Us Desert, northern China, since the Late Holocene. Journal of Arid Land, 8(5): 647–659.

Liu M, Lin Q Z, Wang Q J, et al. 2010. Study on the geochemical anomaly of copper element based on reflectance spectra. Spectroscopy and Spectral Analysis, 5: 1320–1323.

Liu Y, Vekerdy Z. 2003. Possibilities of assessing heavy metal contamination of soil in the Sajo River Flood Plains (Hungary) using reflectance spectroscopy. MSc Thesis. Enschede, Netherlands: International Institute for Geoinformation Science and Earth Observation.

Metelka V, Baratoux L, Jessell M W, et al. 2015. Visible and infrared properties of unaltered to weathered rocks from Precambrian granite-greenstone terrains of the West African Craton. Journal of African Earth Sciences, 112: 570–585.

Middleton M, Närhi P, Kuosmanen V, et al. 2011. Quantification of glacial till chemical composition by reflectance spectroscopy. Applied Geochemistry, 26(12): 2215–2225.

Moumane A, El Ghazali F E, Al Karkouri J, et al. 2021. Monitoring spatiotemporal variation of groundwater level and salinity under land use change using integrated field measurements, GIS, geostatistical, and remote-sensing approach: case study of the Feija aquifer, Middle Draa watershed, Moroccan Sahara. Environmental Monitoring and Assessment, 193: 769, doi: 10.1007/s10661-021-09581-2.

Nair A, Mathew G. 2012. Lithological discrimination of the Phenaimata felsic-mafic complex, Gujarat, India, using the Advanced Spaceborne Thermal Emis-

sion and Reflection Radiometer (ASTER). International Journal of Remote Sensing, 33(1): 198–219.

Pour A B, Park T S, Park Y, et al. 2019. Landsat-8, advanced spaceborne thermal emission and reflection radiometer, and worldView-3 multispectral satellite imagery for prospecting copper-gold mineralization in the Northeastern Inglefield Mobile Belt (IMB), Northwest Greenland. Remote Sensing, 11(20): 2430, doi: 10.3390/rs11202430.

Qian T, Tsunekawa A, Peng F, et al. 2019. Derivation of salt content in salinized soil from hyperspectral reflectance data: A case study at Minqin Oasis, Northwest China. Journal of Arid Land, 11(1): 111–122.

Rathod P H, Müller I, van der Meer F D, et al. 2016. Analysis of visible and near infrared spectral reflectance for assessing metals in soil. Environmental Monitoring and Assessment, 188(10): 558, doi: 10.1007/s10661-016-5568-9.

Rowan L C, Simpson C J, Mars J C. 2004. Hyperspectral analysis of the ultramafic complex and adjacent lithologies at Mordor, NT, Australia. Remote Sensing of Environment, 91(3–4): 419–431.

Sarathjith M C, Das B S, Wani S P, et al. 2016. Variable indicators for optimum wavelength selection in diffuse reflectance spectroscopy of soils. Geoderma, 267: 1–9.

Simandl G J, Paradis S. 2018. Carbonatites: related ore deposits, resources, footprint, and exploration methods. Applied Earth Science, 127(4): 123–152.

Sims D A, Gamon J A. 2002. Relationships between leaf pigment content and spectral reflectance across a wide range of species, leaf structures and developmental stages. Remote Sensing of Environment, 81(2–3): 337–354.

Sracek O, Bhattacharya P, Jacks G. 2004. Behavior of arsenic and geochemical modeling of arsenic enrichment in aqueous environments. Applied Geochemistry, 19(2): 169–180.

van der Meer F D, van der Werff H M A, van Ruitenbeek F J A. 2014. Potential of ESA's Sentinel-2 for geological applications. Remote Sensing of Environment, 148: 124–133.

van der Meer F D. 2018. Near-infrared laboratory spectroscopy of mineral chemistry: A review. International Journal of Applied Earth Observation and Geoinformation, 65: 71–78.

Velasco F, Alvaro A, Suarez S, et al. 2005. Mapping Fe-bearing hydrated sulphate minerals with short wave infrared (SWIR) spectral analysis at San Miguel mine environment, Iberian Pyrite Belt (SW Spain). Journal of Geochemical Exploration, 87(2): 89–103.

Wang Q, Li P, Pu Z, et al. 2011. Calibration and validation of salt-resistant hyperspectral indices for estimating soil moisture in arid land. Journal of Hydrology, 408(3–4): 276–285.

Wang Y, Jia J, Lu H, et al. 2019. Fluvial sediments in the Alagxa Plateau as a dust source: iron mineralogical and geochemical evidence. Journal of Arid Land, 11(2): 217–227.

Wu Y Z, Chen J, Ji J F, et al. 1997. A mechanism study of reflectance spectroscopy for investigating heavy metals in soils. Soil Science Society of America Journal, 71(3): 918–926.

Zeng Y, Hao D, Badgley G, et al. 2021. Estimating near-infrared reflectance of vegetation from hyperspectral data. Remote Sensing of Environment, 267: 112723, doi: 10.1016/j.rse.2021.112723.

Zeraatpisheh M, Ayoubi S, Sulieman M, et al. 2019. Determining the spatial distribution of soil properties using the environmental covariates and multivariate statistical analysis: a case study in semi-arid regions of Iran. Journal of Arid Land, 11(4): 551–566.

Figures

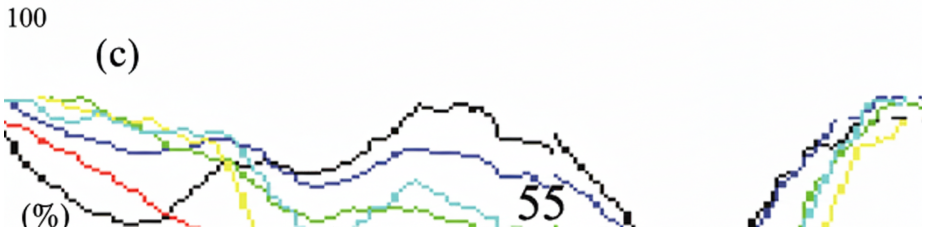

Figure 4: Figure 4